NASA TECHNICAL MEMORANDUM

NASA TM X-68022

NASA TM X-68022

ANALYSIS OF FACE DEFORMATION EFFECTS ON GAS FILM SEAL PERFORMANCE

by John Zuk
Lewis Research Center
Cleveland, Ohio

TECHNICAL PAPER proposed for presentation at
Annual Meeting of the American Society of
Lubrication Engineers
Houston, Texas, May 1-4, 1972

ANALYSIS OF FACE DEFORMATION EFFECTS ON GAS FILM SEAL PERFORMANCE

by John Zuk

National Aeronautics and Space Administration
Lewis Research Center
Cleveland, Ohio

ABSTRACT

Analyses are presented for compressible fluid flow across shaft face seals with face deformation. The solutions are obtained from an approximate integral analysis. The models, used in this analysis, can predict gas film seal behavior operating at subsonic or choked flow conditions. The flow regime can either be laminar or turbulent. Entrance losses can also be accounted for. When fluid inertia effects are negligible (quasi-fully-developed flow) and the sealing faces are slightly deformed, the following results are found for both laminar and turbulent flows: 1) The pressure profiles are independent of fluid properties; 2) The parallel film leakage equation can be used, provided a characteristic film thickness is used. However, fluid inertia effects were found to be very important for near-choked and choked flow conditions. For these conditions the pressure profiles are dependent upon the fluid properties. Pressure profiles are presented for both divergent and convergent seal faces under choked flow conditions.

NOMENCLATURE

A	cross-sectional area, in^2; m^2
C_L	velocity entrance loss coefficient
D	hydraulic diameter, 2h
f	mean Fanning friction factor, $\tau_w \Big/ \frac{\rho u^2}{2}$

h	film thickness (gap), in; m
h_{char}	characteristic film thickness, $(h_1^2 h_2^2/h_m)^{1/3}$, in; m
i	specific enthalpy
M	Mach number
$\dot{M}$	mass flow, lbm/min; kg/sec
P	pressure, psi; N/m^2
R_1	sealing dam inner radius, in; m
R_2	sealing dam outer radius, in; m
$\mathbb{R}$	gas constant, ft-lbf/(lbm)(R); J/(kg)(K)
Re	leakage flow Reynolds number in radial direction, $\rho Uh/\mu$
r	radial direction coordinate
T	linear tilt factor, $h_2^2(2h_1 + \alpha x)/2h_m(h_1 + \alpha x)^2$
T	temperature, F; K
u	mean velocity in r-direction or x-direction, ft/sec; m/sec
W	flow width, in; m
x	coordinate in pressure gradient direction
z	coordinate across film thickness
α	relative inclination angle of surfaces, m rad
β	radial flow factor, W/r
γ	specific-heat ratio
μ	absolute or dynamic viscosity, (lbf)(sec)/in^2; (N)(sec)/m^2
ρ	density, (lbf)(sec^2)/in^4; kg/m^3

subscripts:

char	characteristic
h	based on film thickness
w	wetted surface

0 sealed (reservoir) conditions

1 entrance conditions

2 exit conditions

3 ambient sump conditions

superscripts:

* referenced to Mach one condition (critical flow)

INTRODUCTION

Shaft seals in advanced aircraft rotating machinery will operate at speeds, temperatures, and pressures higher than shaft seals currently used. An example is shaft seals for advanced aircraft turbine engines. Conventional face contact seals presently used in gas turbine engines are limited to sliding velocities of about 350 feet per second (110 m/sec), pressure differentials of about 125 pounds per square inch (86 N/cm^2), and gas temperatures of 800 F (700 K)(1); pressure and speed capabilities of circumferential seals are near that of face seals. Advanced engines, however, will require seals to operate to speeds of 500 feet per second (150 m/sec) (2), pressures to 500 pounds per square inch (340 N/cm^2) and temperatures to 1300 F (980 K)(3). Because of these severe operating conditions, seal face deformation is very likely to occur.

These deformations may be due to various distortions (thermal, centrifugal, pressure, etc.). Seal face distortions become more pronounced under severe operating conditions and are usually detrimental to seal performance. Hence, prediction of these face deformation effects on gas film seal performance is of paramount importance.

For face seals operating under severe conditions, a positive face separation (no rubbing contact) will be required in order to achieve long life and

reliability. A successful method of maintaining positive seal face separation is to add self-acting lift pads, such as shrouded Rayleigh step bearings, to the conventional pressure balanced face seal (4 and 5). This is illustrated in Fig. 1. The self-acting lift pads (gas bearings) have a desirable characteristic, a decrease in film thickness results in an increase in the opening or separating force. Thus, the pads give axial film stiffness to the seal so that the stationary nosepiece will dynamically track with the rotating seal seat. The seal nosepiece must follow the seal seat surface under different operating conditions without surface contact or excessive increase in film thickness, which would yield high leakage. In addition, the self-acting lift pads give the seal a high radial stiffness enabling the seal to accommodate radial face deformations. An experimental investigation of self-acting lift pad performance, where face deformations occured, is reported in (6).

Since the seals must be pressure balanced, a proper balance of the opening forces (due to the pressure drop across the sealing dam and the force generated by the lift pads) and the closing forces (due to hydrostatic forces and spring forces), must be achieved with a leakage gap that has tolerable mass leakage. The gap must be small enough so that the leakage is minimal but it must be large enough so that power dissipation, due to shear in the film, and the inherent face deformations are tolerable. Thus, the design of the sealing gap is vital to seal performance, and the pressure distribution in the gap and mass leakage through the gap must be analyzed.

In this paper, only the sealing dam portion of the seal (Fig. 1) will be analyzed. The classical viscous, isothermal, subsonic, compressible

flow analysis for parallel sealing surfaces is well known (7). Reference (8) analyzed the parallel film constant area hydrostatic case including the effects of fluid inertia, viscous friction and entrance losses. Subsonic and choked flow conditions can be predicted and analyzed for both laminar and turbulent flows. Results showed good agreement with experiment. This paper will extend the analysis of (8) to include seal face deformation effects on the force balance and mass leakage. This analysis should be an aid in both the design of ordinary gas film seals and especially gas film seals with self-acting lift pads.

The objective of the paper is to present mathematical analyses of compressible fluid flow across shaft face seals with face deformations. An approximate integral method will be used to analyze two models. First a quasi-fully developed flow model will be formulated which can be used whenever fluid inertia is negligible (subsonic flow). Secondly, a variable area flow model, where fluid inertia is considered, is shown to be valid for both subsonic and seal exit choked flow. Entrance losses are accounted for and turbulent flow can be analyzed by utilizing an appropriate friction factor-Reynolds number relation.

Causes of Seal Face Deformations

Distortions of the primary sealing faces are inherently present in gas film face seals. Distortions present include radial and axial displacements due to the centrifugal force, and are especially important under high rotational speeds as anticipated for advanced aircraft operation. A typical centrifugal deformation is shown in Fig. 2. Another common face deformation is thermal coning caused by an axial thermal gradient along the shaft. The hotter end of the shaft causes a differential

shaft radial displacement which results in the face coning illustrated in Fig. 3. Other distortions could be caused by: 1) pressure - due to high pressure drops and improper seal balance diameter; 2) mechanical; 3) asymmetry of rotating seal seat; and 4) tolerance buildup due to fabrication and assembly. Generally, for internally pressurized seals, the distortions will cause divergent seal faces.

Basic Model

The sealing dam model (Fig. 4) consists of two coaxial circular rings separated by a very narrow gap. The sealing surfaces are radially deformed. A pressure differential exists between the rings' inner and outer radii. The fluid velocities are small in both the inner-diameter cavity and outer-diameter cavity which bound the sealing dam.

It is essential to have very flat and parallel surfaces for satisfactory gas film seal operation (e.g., specified flatness of the sealing surface within two light bands of sodium). This is necessary to minimize operating distortions. Heat transfer analyses and subsequent stress analyses indicate that relative face deformations of less than two milliradians can be expected (see (5)). Hence, the analysis is representative of small face deformations or tilts. Although the face deformation is never in reality strictly linear, a linear deformation will be assumed since a closed form explicit solution can be readily obtained in some special cases. In practice, no two designs would ever have the same deformation anyway. However, the effect of relative surface deformation can be represented by an "effective" or "apparent" linear tilt of the surface.

As shown in Fig. 4, the effective tilt or deformation of the surface can be represented by a relative tilt angle, α, or by specifying the entrance

and exit film thickness. As shown in Fig. 4, for small linear tilts of the sealing faces, the film thickness at any distance along the leakage flow path X can be found from

$$h = h_1 + \alpha x \qquad [1]$$

where

$$\alpha = \frac{h_2 - h_1}{R_2 - R_1} \qquad [2]$$

Analysis

Two models will be examined and formulated which will predict seal behavior where an exact differential analysis model (9) is impossible to solve or impractical for design analysis purposes. Such cases are turbulent flow, where exact physical knowledge is unknown, and near-choked and choked flow where nonlinear behavior characterizes the flow. Approximate integrated average methods will be used. Although the integral models only satisfy mean conditions in the flow field, they may give good results on gross quantities such as seal leakage and pressure distribution. The constant area analysis (8) used an approximate integrated average method and showed good agreement with experiment.

First a quasi-fully developed compressible flow model will be presented for both parallel and small linear deformed surfaces. This model yields tractable solutions in relatively simple forms. Then a variable area analysis will be formulated for radial area expansion and small surface deformations. This analysis will also include both the quasi-fully developed flow and constant area flow as special cases but the solutions will require a numerical Runge-Kutta solution. (The constant area analysis (8) used a linear iteration solution scheme.)

Quasi-fully Developed Flow Model

This is the classical fluid flow case. This model is widely used to describe pipe and duct flows. This model is valid whenever the viscous forces dominate. That is, when entrance effects are negligible and the flow is subsonic (not near-choked or choked). This flow can be called quasi-fully developed and is presented here from a seal point of view.

Consider the control volume shown in Fig. 5 for situations when the fluid inertia is negligible. The momentum conservation is a balance between the pressure and viscous friction force which is

$$A dP = - \tau_w dA_w \qquad [3]$$

Now introduce the following parameters

$$\text{hydraulic diameter, } D = \frac{4A}{\frac{dA_w}{dx}}$$

$$\text{mean Fanning friction factor, } \bar{f} = \frac{\tau_w}{\frac{\rho u^2}{2}}$$

into Eq. [3] this results in

$$D \frac{dP}{dx} = - 2\rho u^2 \bar{f} \qquad [4]$$

Substituting the perfect gas law and mass flow definition

$$\dot{M} = \rho u A \qquad [5]$$

yields the following useful form

$$P \, dP = \frac{-2\bar{f} \mathcal{R} T \dot{M}^2 \, dx}{DA^2} \qquad [6]$$

Constant Area Flows

Before analyzing sealing surfaces with deformed faces, several constant area cases will be solved. Assuming isothermal flow, constant area, mean friction factor, and hydraulic diameter, Eq. [6] can be readily integrated. The result is

$$\dot{M} = \sqrt{\frac{DA^2\left(P_1^2 - P_2^2\right)}{4\bar{f}\,\mathbb{R}T(R_2 - R_1)}} \qquad [7]$$

For radial flow between co-axial parallel disks and parallel plates, the hydraulic diameter, D, is given by

$$D = 2h \qquad [8]$$

Generally, the mean friction factor is related to Reynolds number by a relation of the following form

$$\bar{f} = \frac{k}{Re^n} \qquad [9]$$

It is useful to express the Reynolds number in the following form

$$Re = \frac{2\dot{M}}{W\mu} \qquad [10]$$

Now, both laminar and turbulent flow cases will be considered.

1) Laminar Flow

For laminar flow, the friction factor is derived from the classical, viscous compressible flow solution (9) and the derivation is also shown in (9). The resulting mean friction factor - Reynolds number relation is

$$\bar{f} = \frac{24}{Re} \qquad [11]$$

Using relation Eq. [10] yields the following form for Eq. [6]

$$P\,dp = \frac{-12\mu\,\mathbb{R}T\,\dot{M}}{Wh^3}\,dx \qquad [12]$$

This equation is identical to a form which can be derived from the differential analysis (9).

2) Turbulent Flow

The Blasius relation of friction factor - Reynolds number appears to satisfactorily describe a large class of fully developed flows. Thus, in Eq. [9], k = 0.079 and n = 0.25. Substitution in Eq. [7] yields

$$\dot{M} = \frac{3.169\ Wh^{12/7}\left(P_1^2 - P_2^2\right)^{4/7}}{\mathcal{R}^{4/7} T^{4/7} \mu^{1/7} (R_2 - R_1)^{4/7}} \qquad [13]$$

which gives the functional relation of the variables in quasi-fully developed turbulent flow.

The pressure distribution can be found by integrating Eq. [6] from the entrance to any distance downstream, x. The result is

$$P_x = \sqrt{P_1^2 - \frac{0.1329\ \mu^{1/4} \mathcal{R} T\, \dot{M}^{7/4} x}{W^{7/4} h^3}} \qquad [14]$$

This equation can be further simplified by substitution of the mass flow Eq. [13]. This yields

$$P_x = P_1 \left\{ 1 + \left[\left(\frac{P_2}{P_1} \right)^2 - 1 \right] \frac{x}{(R_2 - R_1)} \right\}^{1/2} \qquad [15]$$

By examining Eq. [15], we see that the pressure distribution equation is the same as the one for laminar flow (9) and independent of fluid properties. This suggests that it may be desirable from a leakage point of view to operate (if possible) in the turbulent flow regime. (For the same gap the pressure distribution is the same but the leakage is less.)

Variable Area Flows

Eq. [6] can be integrated for both radial flow and constant width flow with small tilts of the sealing surfaces. Using the same restrictions as previously stated the following results are obtained for mass flow:

1) Radial Flow, $W = \beta r$

(a) Laminar flow

$$\dot{M} = \frac{\beta h^3 \left(P_2^2 - P_1^2\right)}{24 \mu \mathbb{R} T \ln R_1/R_2} \qquad [16]$$

Note, that if $\beta = 2\pi$, Eq. [16] becomes the same as the classical viscous, compressible, radial flow leakage equation found in (9).

(b) Turbulent flow

$$\dot{M} = \frac{3.995\ \beta\ h^{12/7} \left(P_1^2 - P_2^2\right)^{4/7}}{\mu^{1/7} \mathbb{R}^{4/7} T^{4/7} \left(\frac{1}{R_1^{3/4}} - \frac{1}{R_2^{3/4}}\right)^{4/7}} \qquad [17]$$

2) Flows With Small Linear Tilts and Constant Width,

$h = h_1 + \alpha x$

(a) Laminar flow

$$\dot{M} = \frac{W h_{char}^3 \left(P_1^2 - P_2^2\right)}{24 \mu \mathbb{R} T (R_2 - R_1)} \qquad [18]$$

This equation is identical to the compressible viscous flow solution obtained from the differential analysis (9). The characteristic film thickness, h_{char}, is defined as

$$h_{char} = \left(\frac{h_1^2 h_2^2}{h_m}\right)^{1/3} \qquad [19]$$

Note when there are no tilts present $h_1 = h_2$ (hence $\alpha = 0$), then $h_{char} = h$ and the classical parallel surface mass leakage equation is evolved. However, if the effect of an effective or linear apparent tilt is desired, the effect on mass leakage can be easily calculated from the parallel leakage equation. A simple computation enables leakage with deformation to be readily calculated or read from a parallel leakage plot.

For this case the radial pressure distribution across the sealing dam is

$$P = P_1 \left\{ 1 + \frac{\left[\left(\frac{P_2}{P_1} \right)^2 - 1 \right] x}{R_2 - R_1} \top \right\}^{1/2} \qquad [20]$$

Where the linear tilt factor, $\top$, is defined as

$$\top = \frac{h_2^2 (2h_1 + \alpha x)}{2h_m (h_1 + \alpha x)^2} \qquad [21]$$

Note for parallel surfaces $\alpha = 0$, hence $h_m = h_1 = h_2$ and the tilt factor, $\top = 1$ which yields the parallel surface pressure distribution.

(b) Turbulent Flow

$$\dot{M} = \frac{3.169 \, W h_{char}^{12/7} \left(P_1^2 - P_2^2 \right)^{4/7}}{\mu^{1/7} \mathcal{R}^{4/7} T^{4/7} (R_2 - R_1)^{4/7}} \qquad [22]$$

This Eq. [22] is identical to Eq. [13] for constant area and parallel surfaces except the characteristic film thickness again describes the small linear tilts.

It is interesting to note that pressure profiles found with small face deformations present are still independent of fluid properties. However,

as will be seen in the next section, this will not be the case when convective inertia effects are important.

Variable Area Flow With Inertia

The objective of this section is to present a mathematical analysis that includes fluid inertia, viscous friction, entrance losses, subsonic and choked flow conditions with area changes due to both radius change and/or small tilts. For subsonic viscous flows the analysis in the previous section can be used; however, with fluid inertia effects the following analysis must be used. The analysis will parallel that for the constant area flow in (8); however, it will be seen that resulting equation to be solved is more complex. The resulting friction parameter, Mach number, and area change equation must be solved using a numerical solution scheme. The numerical scheme used here is the Runge-Kutta technique.

The analysis can be separated into two parts, which can then be considered separately. One part is an analysis of the entrance flow, while the other part is an analysis of the seal leakage path itself.

Entrance Flow

The entrance flow is treated identically as it was for constant area flow (8). That is, the entrance conditions are considered either isentropic or modified to account for entrance losses by an empirically determined velocity loss coefficient, C_L. For example, the entrance pressure can be found from

$$P_1 = \frac{P_0}{\left(1 + \frac{(\gamma - 1)M_1^2}{2C_L^2}\right)^{\gamma/\gamma-1}} \qquad [23]$$

Further details can be found in (8). For subsonic flows where fluid inertia is not important, such as the quasi-fully developed flow, the entrance conditions were shown to be negligible (8)(here $P_0 \cong P_1$). However, entrance effects are important for choked flow conditions.

Seal Leakage Passage Flow

It is assumed that the flow in the seal leakage flow region behaves as a variable area adiabatic flow with friction. A quasi-one-dimensional approximation is made wherein it is assumed that the flow properties can be described in terms of their cross-sectional averages.

The following assumptions have been made in the analysis: 1) The effects of rotation are neglected. 2) The flow is adiabatic. 3) No shaft work is done on or by the system. 4) No potential energy gradient is present such as caused by elevation differences, etc. 5) The fluid behaves as a perfect gas.

The control volume is shown in Fig. 5. The governing equations with area changes reduce to the following differential forms:

Conservation of Mass

$$\frac{d\rho}{\rho} + \frac{1}{2}\frac{du^2}{u^2} + \frac{dA}{A} = 0 \qquad [24]$$

Conservation of Energy

$$\frac{dT}{T} + \frac{(\gamma - 1)}{2} M^2 \frac{du^2}{u^2} = 0 \qquad [25]$$

Equation of State

$$\frac{dP}{P} = \frac{d\rho}{\rho} + \frac{dT}{T} \qquad [26]$$

Conservation of Momentum (for a small area change)

$$-AdP - \tau_w dA_w = \dot{M}du \qquad [27]$$

Introducting the hydraulic diameter and Fanning friction factor into Eq. [27] and combining Eqs. [24], [25], [26], and [27] results in a single equation to be solved which is

$$\frac{dM^2}{M^2} = \frac{-2\left[1 + \frac{1}{2}(\gamma - 1)M^2\right]}{1 - M^2}\frac{dA}{A} + \frac{4fdx}{D}\left[\frac{\gamma M^2\left[1 + \frac{1}{2}(\gamma - 1)M^2\right]}{1 - M^2}\right] \qquad [28]$$

This is the identical result obtained from the Table of Influence Coefficients for generalized one-dimensional flow in (11) and (12).

The dependent variables can be found by integrating directly from M to $M^* = 1$, (A to A^*, etc.) since the variables are separated. Details can be found in (9) and (12). Performing the integrations results in the following equations: (Here the "starred" quantities denote the critical flow conditions.)

$$\frac{u^*}{u} = \frac{1}{M}\sqrt{\frac{1 + \frac{1}{2}(\gamma - 1)M^2}{\frac{1}{2}(\gamma + 1)}} \qquad [29]$$

$$\frac{T^*}{T} = \frac{1 + \frac{1}{2}(\gamma - 1)M^2}{\frac{1}{2}(\gamma + 1)} \qquad [30]$$

$$\frac{\rho^*}{\rho} = \frac{AM}{A^*}\sqrt{\frac{\frac{1}{2}(\gamma + 1)}{1 + \frac{1}{2}(\gamma - 1)M^2}} \qquad [31]$$

$$\frac{P^*}{P} = \frac{A}{A^*M}\sqrt{\frac{\frac{1}{2}(\gamma + 1)}{1 + \frac{1}{2}(\gamma - 1)M^2}} \qquad [32]$$

Solution Scheme

The solution scheme is similar to the constant area case in (13) and will only be briefly described here. Basically the only known boundary

condition is that the flow is critical at some critical film thickness h^*. Hence, h^* is first determined. Then for $h < h^*$, the flow is assumed to be subsonic and for $h > h^*$, the flow is assumed to be choked. The values of h and h^* considered are the characteristic film thickness, h_{char}. The entrance flow must match the seal passage flow. Hence, an iteration scheme must be used. The details of this procedure can be found in (13).

Equation [28] must be solved numerically for the variable area cases of interest. The four point Runge-Kutta scheme is employed. Equation [28] is a first order differential equation in x. Therefore, one boundary condition on M^2 is required. The only known boundary condition is at $x = x^*$, $M^2 = 1$. Hence, a fictitious length must be used for subsonic flow. It would be ideal to start at x^* and march backward to $x = 0$; unfortunately, the derivative dM^2/dx must be known at x^*. Since the derivative is infinite at x^*, this location cannot be used as the starting point. The entrance at $x = 0$ is used as the starting point. An M_1 is guessed which will give $M^* = 1$ at x^*.

The interval of integration is divided into subintervals. Since the Mach number is known to greatly vary in the last 10 percent of the seal prior to the choking point, the last subinterval is divided into smaller subintervals. Further details of this method can be found in (9).

Results and Discussion

Since experimental results are not known to exist for deformed seal surface flow under near-choked and choked flow conditions, some results will now be presented which were obtained from the variable area analysis. Both small linear tilts and pure radial area expansion flow will be considered. (The analysis can be used for monotonically increasing or decreasing

film thickness distributions which would be a specified input.) All results presented here used isentropic entrance conditions and were in the laminar flow regime. The mean friction factor-Reynolds number relation given by Eq. [11] was used in the cases studied. The solutions were obtained using the Lewis Research Center IBM 7094/7040 direct couple computing system.

The approximate integral analysis was first used to solve a class of small surface deformation problems where the viscous differential model (9) was valid. The approximate integral and differential analysis showed good agreement.

Figure 6 compares the pressure profiles obtained from using this analysis with the viscous flow solution using Eq. [20] for a convergent seal face deformation. The conditions used in this analysis are representative of aircraft engine idle and are the same conditions used in the design example in (10). The conditions were: P_0 = 65 psia (45 N/cm^2 abs), P_3 = 15 psia (10.3 N/cm^2 abs), T_0 = 100 F (311 K), R_1 = 2.315 in (5.880 cm), and R_2 = 3.315 in (8.410 cm). The mean film thickness is 0.3 mils (7.6 μm). Notice that there is excellent agreement between the two solutions along the first 40 percent of the seal leakage path (represented by a radial distance from 0 to 0.020 in). Deviation from the small tilt analysis increases as the exit (0.050 in radial distance) is approached (the exit pressure, however, is held fixed as a boundary condition). This result is expected physically. In the first part of the seal leakage passage the flow is still primarily viscous; however, the flow tends to accelerate as it flows towards the exit. Hence, the fluid inertia effects become a concern and the two solutions are not expected to agree in this region.

Figure 7 again shows pressure distribution results obtained from the variable area approximate analysis for a divergent tilt of 2 milliradians. Distributions for mean film thicknesses of 0.1 mil (2.5 μm), 0.2 mil (5.1 μm), 0.3 mil (7.6 μm), and 0.5 mil (12.7 μm) are presented. The other conditions were P_0 = 215 psia (148 N/cm^2 abs), P_3 = 15 psia (10.3 N/cm^2 abs), T_0 = 800 F (700 K), R_1 = 3.265 inch (8.300 cm), R_2 = 3.315 inch (8.410 cm). These conditions are representative of advanced aircraft cruise conditions (10). These conditions represent subcritical (subsonic), critical ($P_2 = P_3$ and $M_2 = 1$) and supercritical (choked) flow conditions. Also shown is the parallel film pressure profile for 0.1 mil (2.5 μm) film thickness. This is the classical parabolic profile for viscous compressible flow. In addition, Fig. 7 shows a supercritical flow pressure profile for parallel sealing surfaces and a film thickness of 0.5 mil (12.7 μm) which was obtained using the constant area analysis of (8). The variable area approximate analysis shows excellent agreement with this parallel film profile with a 0.5 mil (12.7 μm) film thickness.

Figure 8 shows the pressure distribution results obtained from the variable area approximate analysis under identical conditions as those in Fig. 7 except a convergent tilt of 2 milliradians is considered. The parallel film pressure profiles are again presented as a reference. For critical flow the convergent film pressure profile indicates a substantially higher opening force than the parallel film profile. Notice that the variable area analysis again agrees with the constant area analysis case for the supercritical flow case and a 0.50 mil (12.7 μm) parallel film.

Other values of interest in gas film seal design are opening force, center of pressure and leakage flow rates. Table 1 shows the opening force,

center of pressure and entrance and exit Mach numbers for these divergent, parallel and convergent sealing face conditions. These values are for an operating point representative of an advanced aircraft under cruise conditions. Table 2 shows a mass leakage rate comparison for all three sealing surface cases. Both the divergent and convergent seal surface cases have the same characteristic film thickness but the leakage rates are not identical, as is the case when the viscous forces dominate (classical viscous compressible flow). The convergent film case always has less leakage than the divergent film. This is due to the fluid inertia effect which is more pronounced for the convergent film where the fluid accelerates more rapidly than the fluid decelerates in the divergent film case. Also shown in Table 2 is the parallel film case where the mean film thickness equals the characteristic film thickness. The 0.500 mil (12.7 μm) mean film thickness case, only, is close to the tilt cases' characteristic film thickness of 0.497 mils (12.6 μm). Here the leakage for the parallel film is about half the difference of the convergent and divergent seal surface cases.

Figure 9 shows the pressure distribution for pure radial viscous flow found from this variable area approximate analysis and the solution using Eq. [16]. The conditions were representative of aircraft idle operation: P_0 = 65 psia (45 N/cm^2 abs), P_3 = 15 psia (10.3 N/cm^2 abs), T_0 = 100 F (311 K), R_1 = 2.315 inch (5.880 cm), and R_2 = 3.315 inch (8.410 cm). The parallel surface case of 0.50 mil (12.7 μm) film thickness was solved. The variable area approximate analysis slightly underestimates the pressure along the seal passage length. This slight discrepancy is probably due to the choice of mean friction factor. The mean friction factor used here was the same as used for the constant area cases but referenced at the mean

radius. A problem arises in the selection of a mean friction factor for variable area flows. In pure radial flow the mean friction factor varies with radius (since the Reynolds number varies with radius). The proper choice of this friction factor has to be examined in further detail experimentally. The friction factor - Reynolds number relation selection will also be a problem for large surface tilts and should also be investigated experimentally.

As stated in (8), in most face seals the area expansion is negligible due to the radius ratios being close to one. Hence, the flow will usually choke at the exit. However, choking can occur at entrance. If there is a separation bubble present at the entrance (due, e.g., to the flow turning into the sealing faces), there could be a large entrance area decrease with choking occurring at the vena contracta. In this case the analysis presented here cannot be used in its present form. For smaller radius ratios such as those that characterize externally pressurized gas bearings, choking will also occur at the entrance.

SUMMARY OF RESULTS

Approximate integral analyses have been presented for compressible fluid flow across shaft face seals with small face deformations. The fluid properties are averaged across the fluid film. This quasi-one-dimensional integral analysis includes fluid inertia and entrance losses in addition to viscous friction which is accounted for by a mean friction factor. Subsonic and choked flow conditions can be predicted and analyzed. The model is valid for both laminar and turbulent flows. The following pertinent results were found:

Quasi-fully Developed Flow

a) Results for parallel films and small linear tilts agree with the exact classical viscous compressible flow solutions including pure radial flow.

b) Leakage formulas were developed for quasi-fully developed turbulent flow.

c) Small linear tilts of the sealing surfaces can be described using the parallel film leakage equation provided the characteristic film thickness is used. This is true for both laminar and turbulent flows.

d) Pressure profiles are independent of fluid properties for both parallel surfaces and surfaces with small linear tilts. This is true for both laminar and turbulent flow.

Variable Area Flow with Inertia

a) Results agree with pure radial flow results and constant area flows with small seal face deformations.

b) Fluid inertia affects both the pressure distribution and mass leakage flow rates for divergent, convergent, and parallel sealing surfaces. Hence, for severe operating conditions, such as the advanced aircraft cruise conditions considered in this paper, inertia effects must be accounted for to get predictable gas film seal performance.

REFERENCES

1. Parks, A. J., McKibbin, A. H., Ng, C. C. W., and Slayton, R. M., "Development of Mainshaft Seals for Advanced Air Breathing Propulsion Systems," NASA CR-72338 (1967).

2. Shevchenko, R. R., "Shaft, Bearing and Seal Systems for a Small Engine," Paper 670064, SAE (Jan. 1967).

3. McKibbin, A. H., and Parks, A. J., "Aircraft Gas Turbine Mainshaft Face Seals - Problems and Promises," Recent Developments in Seal Technology, ASLE Special Pub. SP-2, 1969, pp. 28-36.

4. Ludwig, L. P., Zuk, J., and Johnson, R. L., "Use of the Computer in Design of Gas Turbine Mainshaft Seals for Operation to 500 Feet per Second (122 m/sec)," Proceedings of the 26th National Conference on Fluid Power, vol. XXIV, 1970, pp. 154-176.

5. Povinelli, V. P., and McKibbin, A. H., "Development of Mainshaft Seals for Advanced Air Breathing Propulsion Systems," Phase II, NASA CR-72737 (June 1970).

6. Hady, W. F., and Ludwig, L. P., "Experimental Investigation of Self-Acting-Lift-Pad Characteristics for Main-Shaft Seal Applications," NASA TN D-6384 (1971).

7. Gross, W. A., "Gas Film Lubrication," John Wiley & Sons, Inc., 1962.

8. Zuk, J., Ludwig, L. P., and Johnson, R. L., "Compressible Flow Across Shaft Face Seals," Proceedings of the Fifth International Conference on Fluid Sealing (1971), Paper FICFS-H6.

9. Zuk, J., "Fluid Mechanics of Gas Film Seals," PH. D. Thesis, Case Western Reserve University (1972).

10. Zuk, J., Ludwig, L. P., and Johnson, R. L., "Design Study of Shaft Face Seal with Self-Acting Lift Augmentation, II - Sealing Dam," NASA TN D-7006, (1970).

11. Shapiro, A. H., "The Dynamics and Thermodynamics of Compressible Fluid Flow," Vol. I, Ronald Press Co., N.Y., 1953.

12. Shapiro, A. H., and Hawthorne, W. R., "The Mechanics and Thermodynamics of Steady, One-Dimensional Gas Flow," Jour. App. Mech., Vol. 14, No. 4 (1947), pp. A317-A336.

13. Zuk, J., and Smith, P. J., "Quasi-One-Dimensional Compressible Flow Across Face Seals and Narrow Slots II - Computer Program," NASA TN E-6305 (1972).

Table 1 - Comparison of various physical quantity values for divergent (+0.002 radian tilt), parallel, and convergent (-0.002 radian tilt) sealing faces representative of subcritical, critical, and supercritical flow; P_0 = 215 p.s.i.a. (148 N/cm^2 abs), P_3 = 15 p.s.i.a. (10.3 N/cm^2 abs), T_0 = 800° F (700 K), R_1 = 3.265 in. (8.300 cm), R_2 = 3.315 in. (8.410 cm). These conditions are representative of an advanced aircraft under cruise operation.

Flow Conditions	Mean Film Thickness, Mils (μm)	Opening Force, lb(kg)			Center of Pressure, % of Total Flow Length			Mach Number					
								Entrance			Exit		
		Tilt Angle, Radians			Tilt Angle, Radians			Tilt Angle, Radians					
		+0.002	0	-0.002	+0.002	0	-0.002	+0.002	0	-0.002	+0.002	0	-0.002
Sub-critical	0.1(2.5)	58(26.3)	133(60.4)	---------	26.0	39.1	------	0.02	0.02	------	0.09	0.25	----
Critical	0.2(5.1)	91(41.3)	135(61.3)	220(100)	33.0	39.7	49.8	0.08	0.07	0.25	0.66	1.00	1.00
Super-critical	0.3(7.6)	106(48.1)	138(62.6)	185(84.0)	36.2	40.5	46.2	0.17	0.14	0.11	1.00	1.00	1.00
Super-critical	0.5(12.7)	119(54.0)	141(64.0)	168(76.3)	40.1	41.7	45.5	0.34	0.29	0.05	1.00	1.00	1.00

Table 2 - Mass leakge rate comparisons found from solutions for divergent tilts (+0.002 radian), convergent tilt (-0.002 radians), and parallel sealing surfaces at film thicknesses representative of subcritical, critical, and supercritical flow; P_0 = 215 p.s.i.a. (148 N/cm^2 abs), P_3 = 15 p.s.i.a. (10.3 N/cm^2 abs), T_0 = 800° F (700 K), R_1 = 3.265 in. (8.300 cm), R_2 = 3.315 in. (8.410 cm)

	Mass Leakage Rate, lbm/min (kg/sec)			
Mean film thickness, h_m, mils (μm)	0.1(2.5)	0.2(5.1)	0.3(7.6)	0.5(12.7)
Characteristic film thickness, h_{char}, mils (μm)	0.0825(2.10)	0.192(4.88)	0.294(7.47)	0.497(12.6)
Flow condition	Subcritical	Critical	Supercritical	Supercritical
Divergent tilt (+0.002 radians)	0.0068(0.0031)	0.0837(0.0380)	0.2800(0.1270)	0.9720(0.4410)
Convergent tilt (-0.002 radians)	----------	0.0827(0.0378)	0.2700(0.1225)	0.9160(0.4160)
Parallel film*	0.0122*(0.0055)	0.0939*(0.0426)	0.2890*(0.1310)	0.9540*(0.4330)

*For a parallel film $h_{char} = h_m$

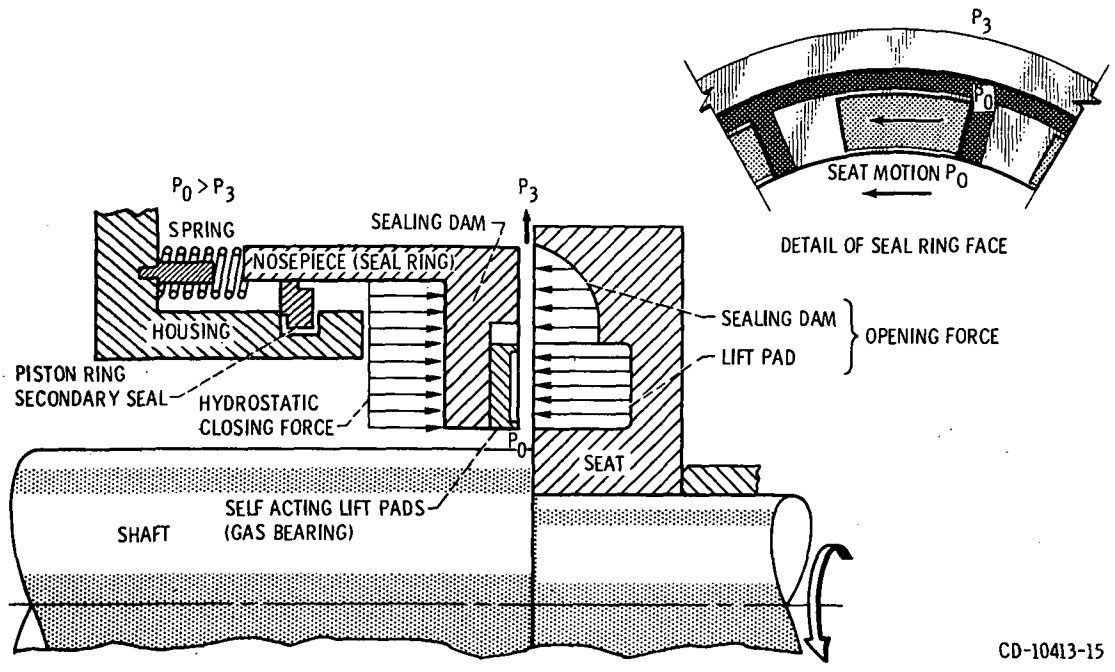

Fig. 1 - Pressure-balanced face seal with self-acting lift pads (added for axial film stiffness).

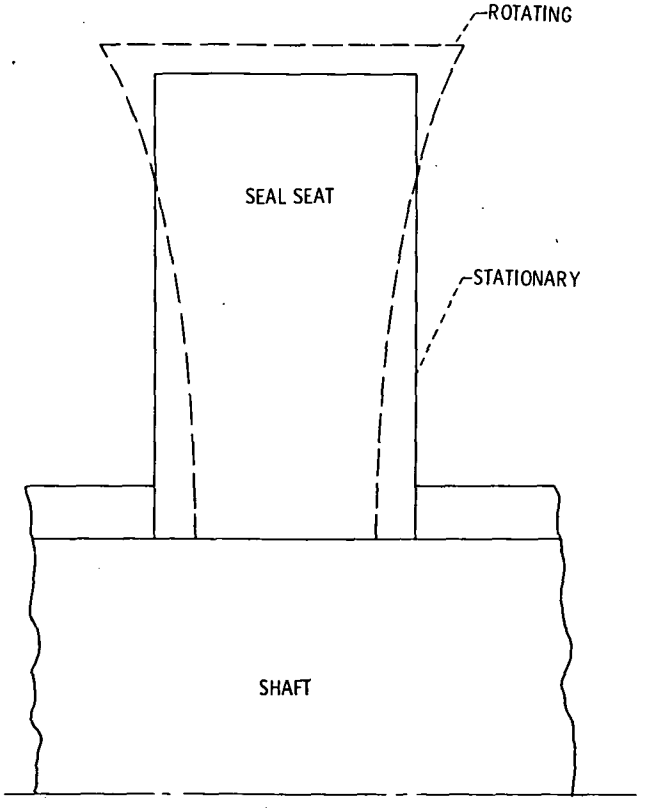

Fig. 2 - Typical distortion of seal seat due to centrifugal force.

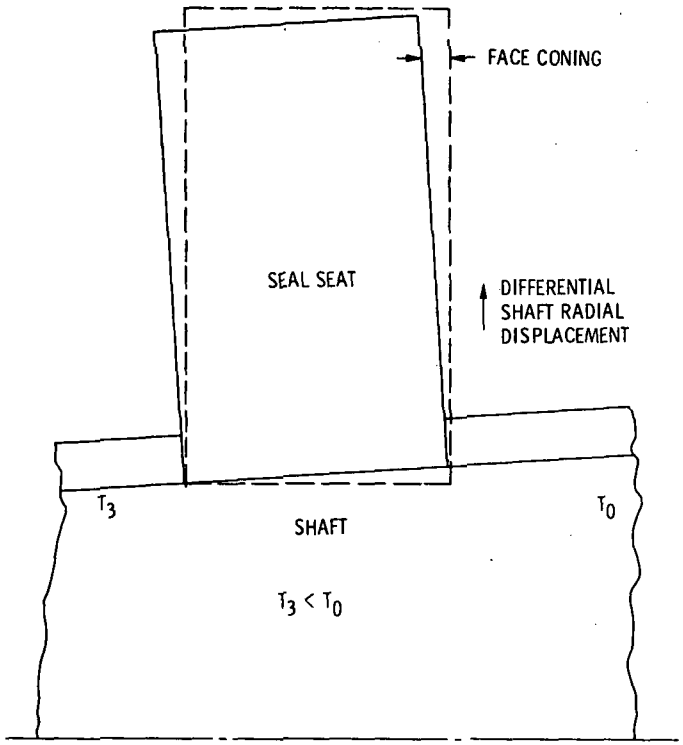

Fig. 3 - Typical thermal distortion of seal due to shaft axial thermal gradient.

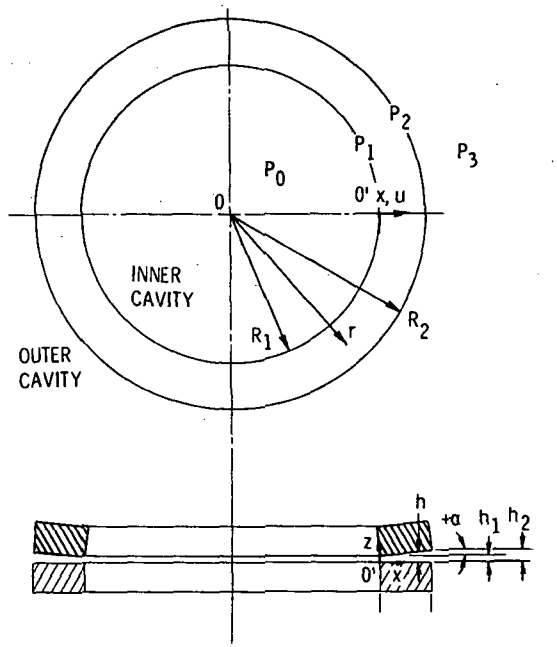

Fig. 4 - Model of the sealing dam with a small tilt angle (not to scale). Upper ring removed for clarity in top view.

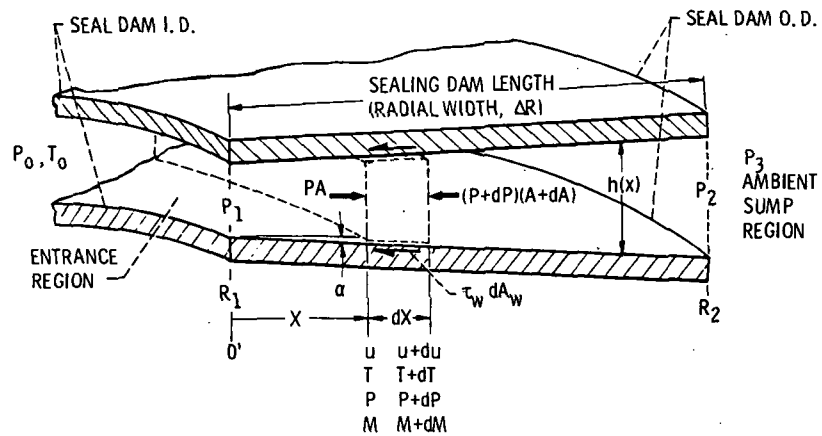

Fig. 5 - Model and notation of sealing faces including control volume for quasi-one-dimensional flow with area change.

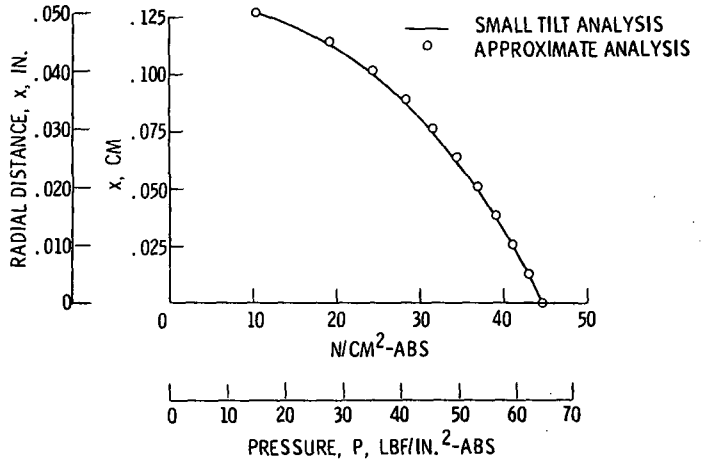

Fig. 6 - Comparison of variable area approximate analysis with exact compressible viscous flow solution; negative one milliradian tilt, 0.3 mil (7.6 μm) mean film thickness, P_1 = 65 psia (45 N/cm^2 abs), 15 psia (10.3 N/cm^2 abs), T_0 = 100^0 F (311 K), R_1 = 3.265 in. (8.300 cm), and R_2 = 3.315 in. (8.410 cm).

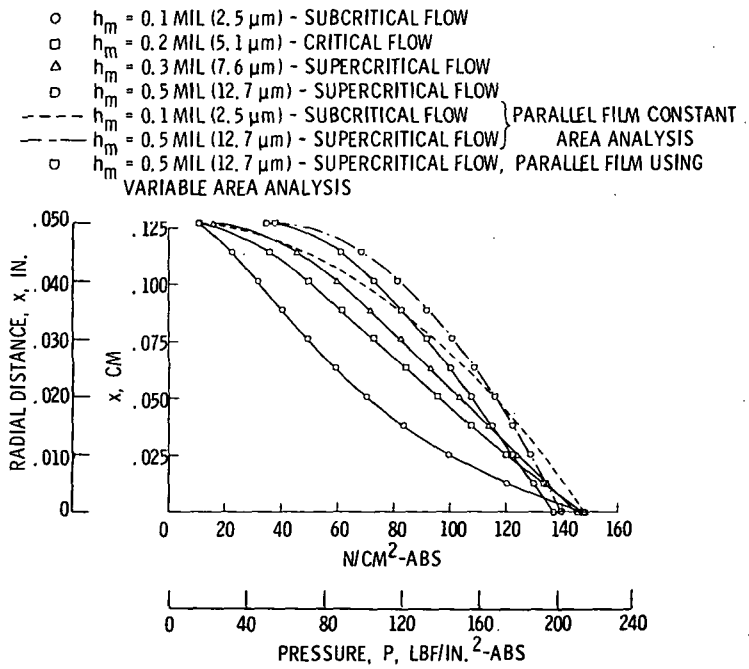

Fig. 7 - Results using the variable area approximate analysis for pressure distributions; positive two milliradian tilt, conditions represent subcritical, critical, and supercritical flow, mean film thicknesses of 0.1 mil (2.5 μm), 0.2 mil (5.1 μm), 0.3 mil (7.6 μm) and 0.5 mil (12.7 μm), P_0 = 215 psia (148 N/cm^2 abs), 15 psia (10.3 N/cm^2 abs), T_0 = 800^0 F (700 K), R_1 = 3.265 in. (8.300 cm), R_2 = 3.315 in. (8.4106 cm). Also shown are comparable parallel film cases.

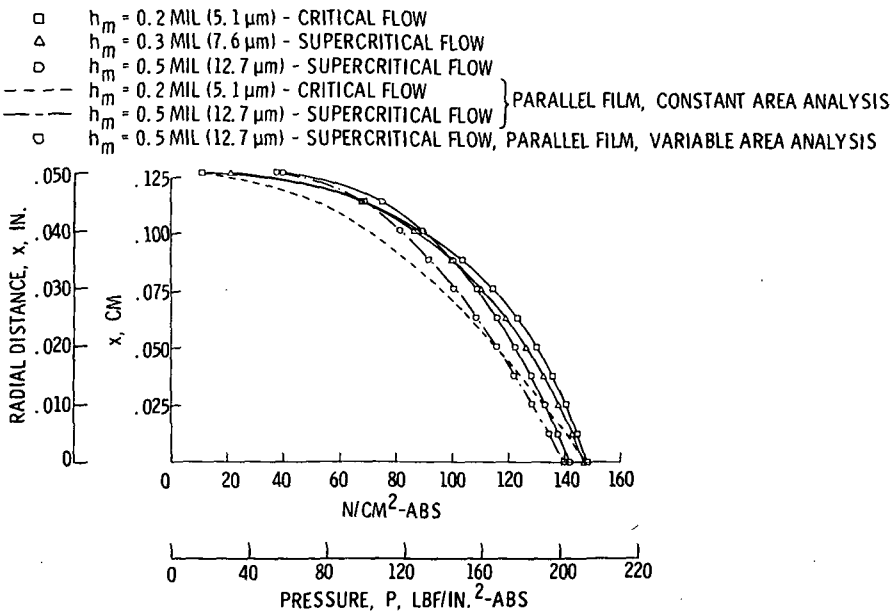

Fig. 8 - Results using variable area approximate analysis for pressure distributions; negative two milliradian tilt, conditions represent subcritical, critical, and supercritical flow, mean film thicknesses of 0.2 mil (5.1 μm), 0.3 mil (7.6 μm), and 0.5 mil (12.7 μm), P_0 = 215 psia (148 N/cm^2-abs), P_3 = 15 psia (10.3 N/cm^2-abs), T_0 = 800° F (700 K), R_1 = 3.265 in. (8.300 cm), R_2 = 3.315 in. (8.410 cm). Also shown are the parallel film cases.

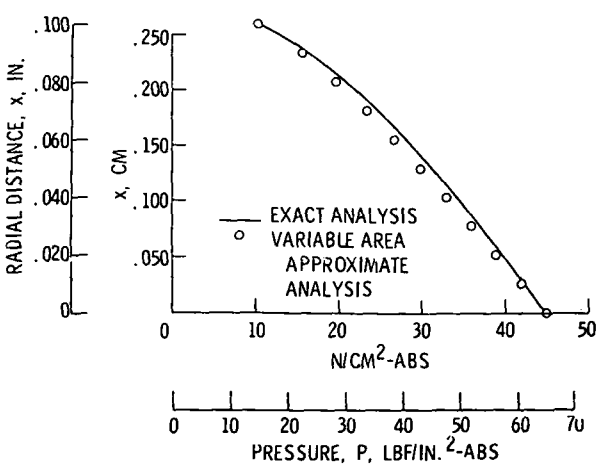

Fig. 9 - Comparison of variable area approximate analysis with exact compressible viscous flow solution for pure radial flow; parallel film, 0.5 mil (12.7 μm) film thickness, P_0 = 65 psia (45 N/cm^2 abs), P_3 = 15 psia (10.3 N/cm^2 abs), T_0 = 100° F (311 K), R_1 = 2.315 in. (5.880 cm), and R_2 = 3.315 in. (8.410 cm).